

# Initial Kinetics of the Direct Sulfation of Limestone

Guilin Hu, Lei Shang, Kim Dam-Johansen, and Stig Wedel

CHEC, Dept. of Chemical Engineering, Technical University of Denmark, 2800 Lyngby, Denmark

Jens Peter Hansen

FLSmidth A/S, 2500 Valby, Denmark

DOI 10.1002/aic.11570

Published online July 22, 2008 in Wiley InterScience (www.interscience.wiley.com).

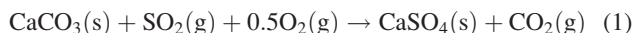
*The initial kinetics of direct sulfation of Faxø Bryozo, a porous bryozoan limestone was studied in the temperature interval from 873 to 973 K in a pilot entrained flow reactor with very short reaction times (between 0.1 and 0.6 s). The initial conversion rate of the limestone—for conversions less than 0.3%—was observed to be significantly promoted by higher SO<sub>2</sub> concentrations and lower CO<sub>2</sub> concentrations, whereas O<sub>2</sub> showed negligible influence. A mathematical model for the sulfation of limestone involving chemical reaction at calcite grain surfaces and solid-state diffusion of carbonate ions in calcite grains is established. The validity of the model is limited to the initial sulfation period, in which nucleation of the solid product calcium sulphate is not started. This theoretical reaction-diffusion model gives a good simulation of the initial kinetics of the direct sulfation of Faxø Bryozo. The intrinsic rate of the direct sulfation of the limestone is estimated to have an activation energy of about 25 kJ/mol and reaction orders of about 0.9 and −0.75 for SO<sub>2</sub> and CO<sub>2</sub>, respectively. The diffusivity of carbonate ions in the surface layer of the calcite grain is estimated to be about three orders of magnitude higher than the diffusivity of carbonate ions in the inner lattice of calcite grain and have an activation energy of about 202 kJ/mol.*

© 2008 American Institute of Chemical Engineers *AIChE J.* 54: 2663–2673, 2008

**Keywords:** sulfation, limestone, kinetics, intrinsic, calcite, solid-state, diffusion

## Introduction

The direct sulfation of limestone is defined as the sulfation reaction between SO<sub>2</sub> and uncalcined limestone and can be expressed by the following overall reaction:



The direct sulfation of limestone is, for example, practically relevant for desulfurization by direct dry sorbent injection dur-

ing pressurized fluid-bed combustion and SO<sub>2</sub> absorption on limestone in the cyclone preheater used in cement production.

The kinetics of the direct sulfation of limestone was studied by a number of authors<sup>1–14</sup> in the past decades. An extensive review of the earlier studies has been done in a recent article by Hu et al.<sup>15</sup> One of the major subjects in the study of the direct sulfation of limestone is the intrinsic kinetics of this reaction. The intrinsic rate data presented in the literature by different authors were either measured at low conversions (for example a few percents) or evaluated by extrapolation to zero conversion with the conversion rate data obtained at relatively high conversions. However, recent study performed by Hu et al.<sup>16</sup> indicates that it is questionable whether those data actually represents the true intrinsic kinetics.

Correspondence concerning this article should be addressed to G. Hu at guh@flsmidth.com.

Hu et al.<sup>16</sup> in another related study demonstrated that the direct sulfation of Faxé Bryozó involves nucleation and crystal grain growth of anhydrite, the solid product. The conversion of the limestone in experiments with long durations showed characteristic two-period behavior with an initial period of a few to 10 s with relatively high but fast-decreasing conversion rate and a second period with relatively low but slow-decreasing conversion rate. The initial period is most likely the period before nucleation of the solid product because the formation of stable product nuclei needs the concentration of sulfate ions at the calcite grain surface to reach a critical level,<sup>17</sup> whereas the second period is the period with crystal grain growth of the solid product. The kinetic properties in these two periods are very different, reflected partly by the large difference in the rates by which the conversion rate decreases with time in these two periods and the sharp transition from the first period to the second period. It has also been shown by Hu et al.<sup>16</sup> that nucleation and crystal grain growth of the solid product can start at a conversion of about 0.5% at temperatures around 873 K. Rate data obtained at conversions significantly higher than, for example, 0.5% represents therefore with high likelihood the kinetics of the period with crystal grain growth of the solid product.

The intrinsic rate of the limestone sulfation is defined as the true chemical reaction rate between the limestone and  $\text{SO}_2$  with the elimination of any influences from diffusion (both gas phase and solid-state diffusion) and the solid product calcium sulfate. As demonstrated by Hu et al.,<sup>16</sup> at conversions of a few percent, the sulfation reaction is significantly hindered by both the resistance of solid-state diffusion and the reduction of directly exposed calcite surface area due to the shielding effect of the formed crystal grains of the solid product, calcium sulfate. Sulfation rates directly measured at conversions of a few percent are therefore with high likelihood significantly lower than the intrinsic rates. Because of the significantly different behavior of the sulfation kinetics in the initial period before nucleation of the solid product and the following period with crystal growth of the solid product,<sup>16</sup> assessing the intrinsic kinetics by simple extrapolation of the rate data obtained at a few percent or higher conversions to zero conversion will easily lead to faulty results.

Cement is currently produced mainly by using the so-called “dry process”. In this process, a cyclone preheater consisting of several cyclones in series (usually 4–5 cyclones) is used to preheat the raw meal (ground raw material mixture) through direct heat exchange between the hot flue gas from the downstream process and the raw meal particles suspended in the gas. The residence time of the raw meal particles in each cyclone is around 10 s. In the hot and oxygen-containing environment in the cyclones,  $\text{SO}_2$  is formed, mainly from oxidation of pyrite contained in the raw meal. Part of the formed  $\text{SO}_2$  is absorbed on the limestone particles—the main constituent of the raw meal—through the direct sulfation of the limestone. The rest gets out of the system together with the flue gas. Absorption of  $\text{SO}_2$  by the limestone particles in the raw meal in the cyclone preheater is desired for both the  $\text{SO}_2$  emission reduction from the production process and the production of cement itself, because calcium sulfate is a needed minor ingredient of cement products. Because of the relatively short residence time of the

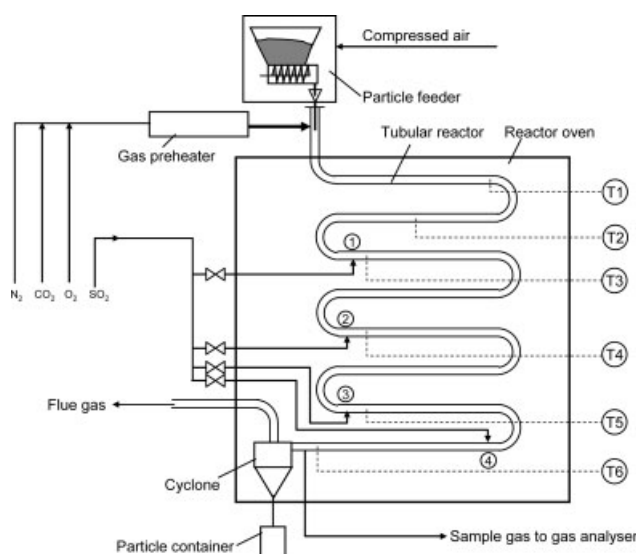


**Figure 1. Illustration of the pilot entrained flow reactor.**

raw meal particles in the cyclones, the initial kinetics of the direct sulfation of limestone is practically important for  $\text{SO}_2$  absorption in the cyclone preheater. In this study, the initial sulfation rates are measured by experimental methods. A mathematical model is established to describe the initial sulfation process and to assess parameters of the intrinsic kinetics as well.

## Experimental

### Reactor set-up

For the purpose of measuring the sulfation rates at near-zero limestone conversion, a pilot entrained flow reactor was built and used for the experiments. As illustrated in Figure 1, the pilot entrained flow reactor system includes a gas supply unit, an electrically heated gas preheater, a particle feeder, a tubular reactor, and a data acquisition system. The required amount of gases ( $\text{SO}_2$ ,  $\text{CO}_2$ ,  $\text{O}_2$ ,  $\text{N}_2$ , and compressed air) are supplied by the gas supply unit.  $\text{SO}_2$ ,  $\text{CO}_2$ , and  $\text{O}_2$  are from the gas cylinders. Compressed air is from the utility supply net. The flow rate of each gas is controlled by a mass flow controller.

Before entering the reactor, the mixed gases ( $\text{CO}_2$ ,  $\text{O}_2$  and  $\text{N}_2$ ) are preheated to the required temperature (usually a couple of hundred degrees higher than the reaction temperature). The limestone particles are fed by the automatic particle feeder at a constant rate to the reactor. Compressed air is used as carrier gas for the particles and as a source of  $\text{O}_2$  for the reaction as well. The preheated gas and the limestone particles meet at the inlet to the reactor. The limestone particles suspended in the gas stream are first heated up by the preheated gas and further heated to the required reaction temperature in the first part of the tube reactor (from the inlet of the reactor to the first  $\text{SO}_2$  injection point).

The reactor is made of Fe-Cr-Ni based high temperature resistant alloy tubing (AVESTA 235MA, DIN 1.4893-X8CrNi21-11) with an outer diameter of 26.7 mm and a wall thickness of 2.11 mm. The total length of the reactor is

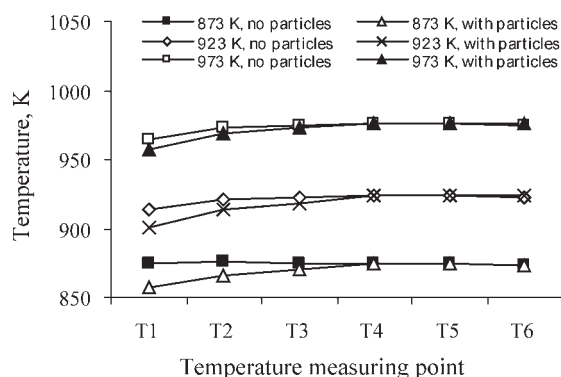


**Figure 2. Temperature profile in the reactor tube with and without the particle feeding.**

about 15 m.  $\text{SO}_2$  from the gas supply unit is injected at one of the four injection points along the length of the reactor. The dosing heads are specially designed with small holes to ensure an even distribution of  $\text{SO}_2$  in the main gas flow. By shifting between the injection points, conversions at different reaction times under identical flow and temperature conditions can be measured.

The temperature in the reactor is monitored at six points along the reactor length. Figure 2 shows the temperature profile without and with the particle feeding at the three reaction temperatures used in the experiments. This figure shows that the temperature in the reactor is quite close to the set point down stream of the first  $\text{SO}_2$  injection point. For experiments at 873 and 923 K, the temperatures at the first  $\text{SO}_2$  injection point was about 3–5 K lower than the set point. This relatively small temperature difference is estimated to have very limited influence on the experimental results obtained with the  $\text{SO}_2$  injected at the first injection point, because this temperature difference, in addition to its small magnitude, is estimated to disappear after about 1/5 of the total reaction time.

The sulfation starts when the heated particles meet  $\text{SO}_2$  at the injection point. After the reaction, the particles are separated in a cyclone that is directly connected to the reactor. The separated particles fall down into the container outside the reactor oven. The gas is sampled just before the cyclone and is analyzed for the concentration of  $\text{SO}_2$ ,  $\text{O}_2$ , and  $\text{CO}_2$  in online gas analyzers. The difference between the  $\text{SO}_2$  outlet concentrations with and without limestone particle feeding is used to calculate the conversion of the limestone at the corresponding reaction time.

Conversion of  $\text{SO}_2$  to  $\text{SO}_3$  at elevated temperatures and especially in a steel reactor is often a concern for the study of kinetics of limestone sulfation. Under the applied reaction conditions in this study, the conversion of  $\text{SO}_2$  to  $\text{SO}_3$  was confirmed to be insignificant, as a gradual increase in the reaction temperature from room temperature up to 973 K without limestone particle feeding showed no significant decrease in the outlet  $\text{SO}_2$  concentration.

### Limestone

The limestone used for the experiments is a soft and porous bryozoan limestone from Faxø Kalk in Denmark

(referred to hereafter as Faxø Bryozo). Faxø Bryozo, in powder form when purchased, was sieved by using a standard sieve and the fraction with particle sizes between 0.063 and 0.18 mm was used for the experiments. The particles of Faxø Bryozo are agglomerates of primary grains of a few micrometers in size.<sup>18–22</sup> The limestone particles were dried at about 393 K for 12 h in an electrically heated oven and then stored in air tight containers. Table 1 shows the properties of Faxø Bryozo.

### Experimental condition

Experiments were carried out in the temperature interval from 873 to 973 K under ambient pressure. The influences of  $\text{SO}_2$ ,  $\text{O}_2$ , and  $\text{CO}_2$  were investigated at two concentrations [ $\text{SO}_2$ : 900 and 1800 ppmv (corresponding to 0.04 and 0.08 mol/ $\text{Nm}^3$ , respectively);  $\text{O}_2$ : 3 and 6 vol % (corresponding to 1.34 and 2.68 mol/ $\text{Nm}^3$ , respectively);  $\text{CO}_2$ : 8 and 15 vol % (corresponding to 3.57 and 6.70 mol/ $\text{Nm}^3$ , respectively)]. A gas velocity of about 20 m/s in the reactor was used in order to ensure a turbulent gas flow. Reynolds number was calculated to be around 5000–6000 at such gas velocity. The solid feeding rate ranges from 0.5 to 2 kg/h, which corresponds to a volumetric solid to gas ratio less than  $6 \times 10^{-5}$  at the used reaction conditions. The applied temperature, pressure, and gas concentrations are all relevant values in the cyclone preheater used in cement production.

### Results and Discussion

The conversion of the limestone was calculated based on the difference between the outlet  $\text{SO}_2$  concentrations without and with limestone particle feeding by using the following equation:

$$x = \frac{P V (y_{\text{SO}_2, \text{no particle feeding}} - y_{\text{SO}_2, \text{with particle feeding}}) M_{\text{CaCO}_3}}{R T w \eta} \quad (2)$$

**Table 1. Properties of Faxø Bryozo Particles Used for the Experiments**

Composition*	97
CaCO <sub>3</sub> (wt %)	
Elemental analysis (wt %)	
Na	<detection limit of 0.001
Mg	0.26
Al	0.026
Si	0.23
P	0.014
S	0.03
K	0.0054
Ca	39
Ti	0.002
V	0.002
Cr	<detection limit of 0.001
Mn	0.02
Fe	0.047
Zn	0.0014
Sr	0.042
Particle size (mm)	0.063–0.18
Total surface area <sup>†</sup> (m <sup>2</sup> /g)	0.79
Porosity <sup>‡</sup>	0.3

\*Determined by wavelength dispersive X-Ray (Philips PW2400).

<sup>†</sup>Determined by BET (Micromeritics ASAP 2000).

<sup>‡</sup>Determined by mercury intrusion (Micromeritics, MicroAutopore II9220).

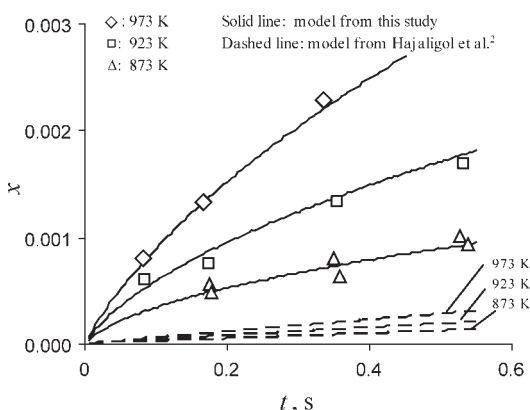


**Figure 3. Variation of conversion of Faxe Bryozo with reaction time at different temperatures (standard conditions if not specified:  $P$ : 0.1 MPa; inlet  $\text{SO}_2$ : 1800 ppmv;  $\text{O}_2$ : 3 vol %;  $\text{CO}_2$ : 15 vol %;  $\text{N}_2$ : balance).**

The markers are experimental data. The lines are model simulations; solid lines: simulations with the model established in this study; dashed lines: simulations with the model from Hajaligol et al.<sup>2</sup>

Based on the measured conversions, the kinetic properties of the initial sulfation process are evaluated and discussed. Two rate concepts are used to represent the sulfation rate of the limestone. One is conversion rate, which has the unit of  $\text{s}^{-1}$  and is defined as limestone conversion achieved per unit time (second). The second is the surface reaction rate ( $r$ ), which has the unit of  $\text{mol}/(\text{m}^2\text{s})$  and is defined as the amount of solid reactant (in mol) reacted per unit time (second) and per unit surface area (square meter). The surface reaction rate is obtained by dividing the conversion rate with the molar total surface area of the limestone particles.

As listed in Table 1, the limestone sample used for the experiments has a total surface area of  $0.79 \text{ m}^2/\text{g}$  or  $79 \text{ m}^2/\text{mol}$  and a porosity of about 30%. According to Froment and Bischoff,<sup>23</sup> the intra-particle diffusion resistance is insignificant when the generalized Thiele modulus is less than 0.5 (corresponding to an effectiveness factor  $>0.95$ ). To check the degree of influence of intra-particle diffusion, the generalized Thiele modulus is calculated for each experiment with the up-limit particle size. The diffusion coefficient of  $\text{SO}_2$  in the gas is estimated by the Fuller, Schettler, and Giddings relation.<sup>24–26</sup> By using the rate data measured at different  $\text{SO}_2$  concentrations in this study, the average apparent reaction order of  $\text{SO}_2$  is calculated to be about 0.4. The generalized Thiele modulus is calculated to be smaller than 0.5 for all the experiments. Considering that the average particle size is significantly smaller than the up-limit particle size of 0.18 mm, the average effectiveness factor should thus be significantly higher than 0.95. Because of the insignificant resistance of intra-particle diffusion and the very low limestone conversions achieved in this study, the calculated surface reaction rate should therefore represent the true sulfation rate at the surface of the solid reactant.

Figures 3–6 show the measured conversions of the limestone at different temperatures, gas concentrations, and reaction times. Due to the relatively small difference between the

two  $\text{SO}_2$  concentrations without and with limestone particle feeding (generally in the interval from 30–70 ppmv), the main error sources of the calculated conversion of the limestone was from measurements of  $\text{SO}_2$  concentrations and gas flow rates. It is estimated that a maximum deviation of approximately  $\pm 2$  ppmv may exist for the measured  $\text{SO}_2$  concentrations and 1% of the total gas flow rates for gas flow measuring. Based on these two major measuring errors, the standard deviations of the measured conversions of the limestone are estimated to be around 5–8%. In the presented figures, the vertical size of the data markers corresponds to the estimated standard deviations. Experiments at the two  $\text{SO}_2$  concentrations (1800 and 900 ppmv) at 873 K were repeated at two different campaigns. As it is seen in the presented figures, except one data point obtained at the reaction time of about 0.37 s and with 1800 ppmv  $\text{SO}_2$  in the gas, the reproducibility of other data points is quite good.

Figure 3 shows the variation of conversion of Faxe Bryozo with time at different temperatures in a gas consisting of 1800 ppmv  $\text{SO}_2$ , 3 vol %  $\text{O}_2$ , 15 vol %  $\text{CO}_2$ , and 81.8 vol %  $\text{N}_2$ . This figure demonstrates clearly the significant increase in the conversion rate of the limestone with increasing temperature. By using the average conversion rates (dividing the conversion by the corresponding reaction time), the apparent activation energies are estimated to be approximately 43, 69, 86, and 74 kJ/mol at reaction times of 0.08, 0.17, 0.35, and 0.53 s, respectively. (The apparent activation energies at the reaction times of 0.08 and 0.53 s are evaluated by using data at two temperatures and therefore may have larger uncertainties than the other two values.)

Figures 4 and 5 show, respectively, the influences of  $\text{SO}_2$  and  $\text{CO}_2$  on the conversion of the limestone at different temperatures. As it is indicated by the obtained conversions shown in these two figures, the conversion rate increases with increasing  $\text{SO}_2$  concentration but decreases with increasing  $\text{CO}_2$  concentration. By using the average conversion rates, the average apparent reaction orders of  $\text{SO}_2$  and  $\text{CO}_2$

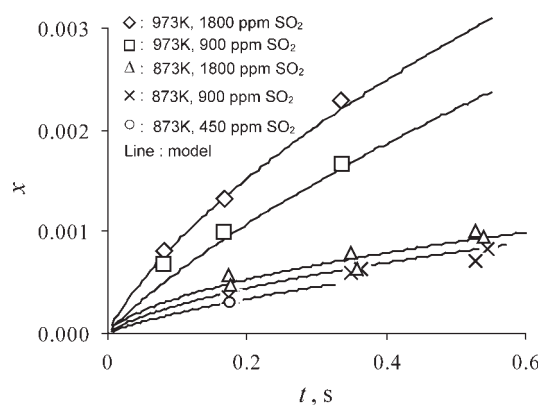


**Figure 4. Variation of conversion of Faxe Bryozo with reaction time at different temperatures and  $\text{SO}_2$  concentrations (standard conditions if not specified:  $P$ : 0.1 MPa;  $\text{O}_2$ : 3 vol %;  $\text{CO}_2$ : 15 vol %;  $\text{N}_2$ : balance).**

The markers are experimental data. The lines are model simulations with the model established in this study.



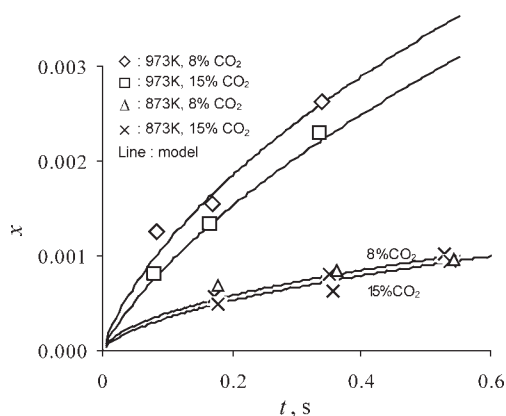


**Figure 5. Variation of conversion of Faxe Bryozo with reaction time at different temperatures and CO<sub>2</sub> concentrations (standard conditions if not specified: *P*: 0.1 MPa; SO<sub>2</sub>: inlet 1800 ppmv; O<sub>2</sub>: 3 vol %; N<sub>2</sub>: balance).**

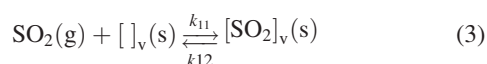
The markers are experimental data. The lines are model simulations with the model established in this study.

are estimated to be around 0.4 and  $-0.3$ , respectively. The effects of SO<sub>2</sub> and CO<sub>2</sub> are in principle similar to the observations made by Hu et al.<sup>16</sup> with the same limestone at significantly longer reaction times.

Figure 6 shows the variation of conversion of Faxe Bryozo with the time at different oxygen concentrations and temperatures. This figure demonstrates that the conversion was not promoted by higher O<sub>2</sub> concentrations in the investigated O<sub>2</sub> concentration interval. This phenomenon is very different from the observed promoting effect of O<sub>2</sub> by Hu et al.<sup>16</sup> with the same limestone at similar O<sub>2</sub> concentrations at significantly longer reaction times.

Hu et al.<sup>16</sup> proposed the following multi-step mechanism for the sulfation reaction:

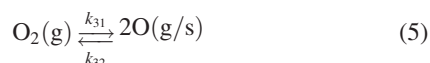
Step 1: adsorption of SO<sub>2</sub> in active sites (suggested to be vacancies of carbonate ions) at the surface of the calcite grains:



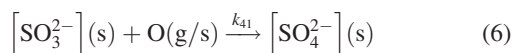
Step 2: conversion of the adsorbed SO<sub>2</sub> to sulfite ions:



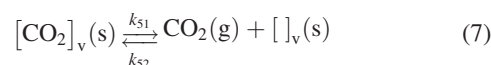
Step 3: formation of oxygen radicals in gas phase or at the solid surface by dissociative adsorption:



Step 4: oxidation of sulfite ions to sulfate ions:



Step 5: desorption of CO<sub>2</sub>:



It was pointed out by Hu et al.<sup>16</sup> that due to the formation of product ions and the significant resistance of solid-state diffusion, the surface layer of the calcite grain is not pure calcite any more. To describe the reaction kinetics, it is necessary to consider the variation of carbonate ion concentration at the calcite grain surface. Based on this mechanism, Hu et al.<sup>16</sup> deduced the following rate equation for the conversion of carbonate ions (equivalent to conversion of the solid reactant) at the calcite grain surface:

$$r = \frac{k_{21}K_1C_{\text{SO}_2}a^s}{1 + K_5^{-1}C_{\text{CO}_2} + K_1C_{\text{SO}_2}} \quad [\text{mol}/(\text{m}^2\text{s})] \quad (8)$$

Here,  $a^s$  is the dimensionless carbonate ion concentration at the calcite grain surface, which is defined as the ratio between the actual carbonate ion concentration at the surface and the carbonate ion concentration in pure calcite crystal.

This rate expression can be understood as the multiplication between the intrinsic rate,  $r^0$  (rate at zero conversion) and the actual dimensionless carbonate ion concentration at the calcite grain surface:

$$r = r^0 a^s \quad (9)$$

Here,

$$r^0 = \frac{k_{21}K_1C_{\text{SO}_2}}{1 + K_5^{-1}C_{\text{CO}_2} + K_1C_{\text{SO}_2}}$$

The above reaction mechanism seems to give satisfactory explanations of the observed special behavior of the initial sulfation kinetics.

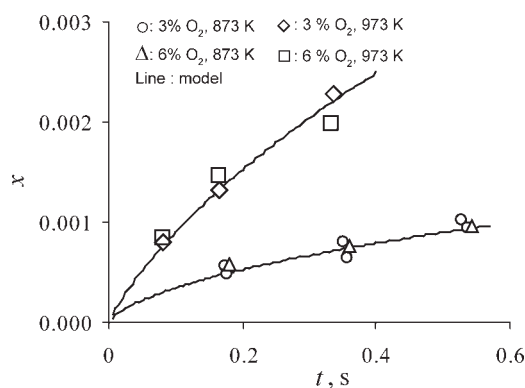


**Figure 6. Variation of conversion of Faxe Bryozo with reaction time at different temperatures and O<sub>2</sub> concentrations (standard conditions if not specified: *P*: 0.1 MPa; inlet SO<sub>2</sub>: 1800 ppmv; CO<sub>2</sub>: 15 vol %; N<sub>2</sub>: balance).**

The markers are experimental data. The lines are model simulations with the model established in this study.

The conversion vs. time data shown in Figures 3–6 demonstrate that the conversion rate of the limestone decreases quickly with increasing reaction time in all the cases. This fast decay of the conversion rate with the reaction time could be explained by a fast decrease in  $a^s$  caused by the significant influence of solid-state diffusion in the initial sulfation period. The generally increasing apparent activation energies with increasing reaction time may be a reflection of the increasing resistance of solid-state diffusion with increasing reaction time or conversion.

The effect of  $\text{SO}_2$  can be explained well by its influence on the intrinsic rate according to Eq. 9. However, the effect of  $\text{CO}_2$  in addition to its influence on the intrinsic rate according to Eq. 9, may also come from its effect on  $a^s$  because of its influence on carbonate ion diffusivity.<sup>16,27–29</sup> Labotka et al.<sup>29</sup> showed that carbonate ion diffusivity increases with decreasing  $\text{CO}_2$  partial pressure.  $a^s$  may thus be higher at a lower  $\text{CO}_2$  partial pressure.

$\text{O}_2$ , according to Eq. 9, apparently does not influence the sulfation rate. According to the mechanism shown above,  $\text{O}_2$  has influence on the conversion of sulfite ions (the intermediate product) to sulfate ions (the final product) in Step 4. In the initial stage, nucleation is not supposed to initiate. The formed intermediate sulfite ions and the final product ions, that is, the sulfate ions take the lattice sites of carbonate ions at the surface of calcite grains and accumulate mostly at the surface because of the relatively low solid-state diffusivity. A small part of the sulfite and sulfate ions may diffuse into the inner part of the calcite grains.  $\text{O}_2$  showed no significant influence at this stage simply because both sulfite and sulfate ions stay mostly at the surface. Formation of more or less sulfate ions does not make noticeable difference.

However, in the period with crystal grain growth of the solid product, the faster conversion of the sulfite ions to the sulfate ions at a higher oxygen concentration may result in a higher limestone conversion rate because the formed sulfate ions will diffuse toward nearby product crystal grains instead of accumulating at the calcite grain surface uncovered by product crystals, which thus results a higher  $a^s$ . This may explain the promoting effect of oxygen after a longer reaction time.

As pointed out in the introduction, assessment of the intrinsic kinetics by extrapolation of the rate data obtained in the period with crystal growth of the solid product may be inappropriate because of the significantly different kinetic properties in the periods before and after nucleation of the solid product. Figure 7 shows a comparison between the average surface reaction rates measured at the shortest residence times (about 0.08 s at 973 K and 923 K, and about 0.17 s at 873 K) in this study and the intrinsic surface reaction rates predicted by intrinsic rate expressions presented in the literature<sup>1,2,5,13</sup>). For the sulfation of Faxa Bryozo conducted in this study, the intrinsic rates are expected to be higher or at least not lower than the measured average rates. As seen in the figure, the rates predicted by the intrinsic rate expressions presented in the literature are about 15–100 times lower than the average surface reaction rates measured in this study. The differences between the true intrinsic rates of the direct sulfation of Faxa Bryozo and the rates predicted by the intrinsic rate expressions presented in the literature are expected to be even larger. This great undershoot by the intrinsic rate expressions presented in the literature supports

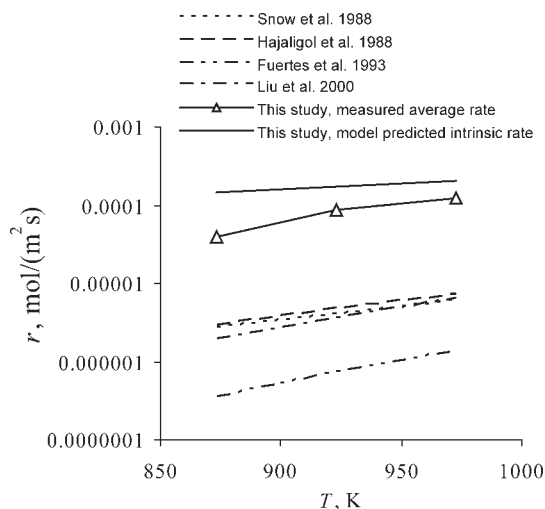


**Figure 7. Comparison of surface reaction rates between values measured at the shortest residence times (about 0.08 s at 973 and 923 K, and 0.17 s at 873 K) in this study, values predicted by the intrinsic rate expressions presented in the literature, and values predicted by the intrinsic rate expression assessed in this study (other conditions:  $P$ : 0.1 MPa;  $\text{SO}_2$ : 1800 ppmv;  $\text{O}_2$ : 3 vol %;  $\text{CO}_2$ : 15 vol %;  $\text{N}_2$ : balance).**

our doubt about the appropriateness of assessing the intrinsic kinetics by the rate data obtained in the period with crystal growth of the solid product.

The experimental conditions used in this study allowed us to measure conversion rates free from the influence of the product crystal growth, although solid-state diffusion resistance could not be eliminated. The intrinsic kinetics is therefore assessed by model simulations.

### Modeling

As proposed by Hu et al.,<sup>16</sup> the initial sulfation reaction takes place at the surface of calcite grains. The product ions such as sulfate ions or sulfite ions formed at the surface diffuse subsequently towards the inner part of the calcite grain, whereas the carbonate ions diffuse towards the surface to participate the reaction. This reaction-diffusion process is illustrated in Figure 8.

The reaction causes a significant decrease in the carbonate ion concentration at the calcite grain surface because of the relatively low solid-state diffusivity, which in turn results in a significant decrease in the sulfation rate. The effect of the carbonate ion concentration at the calcite grain surface on the sulfation rate is accounted by the parameter  $a^s$  in Eq. 9. Under non-steady state conditions,  $a^s$  is a function of time. If  $a(l, t)$  designates the dimensionless carbonate ion concentration in the calcite grain at time  $t$  and a distance of  $l$  from the grain surface, then Eq. 9 can be rewritten as follows:

$$r = r^0 a(0, t) \quad (10)$$

Here,  $a(0, t)$  is the dimensionless carbonate ion concentration at the calcite grain surface at time  $t$ .

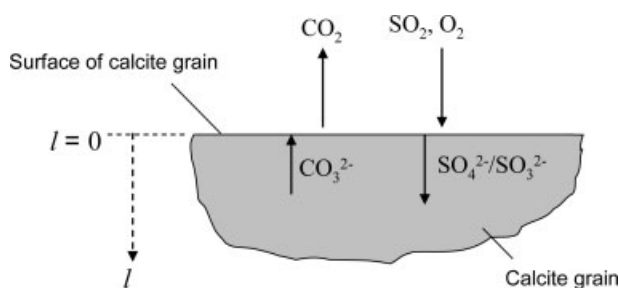


**Figure 8. Illustration of the reaction-diffusion process before the initiation of the nucleation of the solid product.**

Ionic diffusion in the calcite grain involving  $\text{CO}_3^{2-}$ ,  $\text{SO}_4^{2-}$  and most likely also  $\text{SO}_3^{2-}$  can be assumed to be equi-molar because solid-state ionic diffusion takes place by point defects<sup>30,31</sup> and electroneutrality is required. Fick's law is widely used to describe solid-state ionic diffusion.<sup>32–36</sup> Calculations indicate that the diffusion treated in this study takes place in a relatively thin layer of about 5–10 nm (corresponding to about 15–30 layers of carbonate ions in calcite crystal lattice) near the calcite grain surface. It is assumed that Fick's law is still applicable in such a thin layer-thickness. Because of this relatively thin layer-thickness, it is also sufficient to assume slab geometry for mathematical treatment.

The solid-state diffusivity of carbonate ions ( $D_s$ ) may vary with factors such as temperature,  $\text{CO}_2$  concentrations,<sup>27–29</sup> and solid composition, which varies with the conversion of the calcite grain. However, due to limitations of experimental conditions in this study it is not able to consider the influence of  $\text{CO}_2$  concentration and solid composition separately. It is assumed that the solid-state diffusivity of carbonate ions ( $D_s$ ) varies only with temperature. This is, of course, a simplified treatment.

With the above assumptions, a mass balance concerning the diffusion of carbonate ions in a thin layer near the calcite grain surface leads to the following partial differential equation with one initial condition and two boundary conditions:

$$\frac{\partial a(l,t)}{\partial t} = D_s \frac{\partial^2 a(l,t)}{\partial l^2} \quad (11)$$

$$\text{IC1: } a(l,0) = 1 \quad (12)$$

$$\text{BC1: } a(l,t) = 1 \quad \text{when } l \rightarrow \infty \quad (13)$$

$$\text{BC2: } \frac{\partial a(0,t)}{\partial l} = \left( \frac{1}{D_s C_{\text{CO}_3^{2-}}^0} \right) r^0 a(0,t) \quad (14)$$

IC1 is simply a statement that no calcite has reacted at  $t = 0$ .

BC1 is an idealization, stating that the solid reactant (calcite) is not reacted at a distance sufficiently far from the surface. In our case, calculations indicate that this condition is fulfilled when  $l$  is larger than about 10 nm, mainly because of the very short reaction time and slow solid-state diffusion.

BC2 is the key condition in this model because it relates the reaction at the surface to the diffusion process in the

grain. BC2 is claimed by assuming that the diffusion rate of carbonate ions at the calcite grain surface is equal to the consumption rate of carbonate ions by the reaction at the calcite grain surface.

Equation (11) was solved with Maple 10 from Maplesoft by using the centered time and centered space method (Crank Nicholson method).

In our case, BC1 is fulfilled by performing the calculation in a thin slab with a thickness larger than 10 nm, as calculations demonstrated that the results do not vary with the slab thickness when the thickness is larger than 10 nm. 20 nm was the slab thickness practically used for all the calculations.

The conversion of the limestone particles can be calculated by the following equation:

$$x = \int_0^t S_t M_{\text{CaCO}_3} r^0 a(0,t) dt \quad (15)$$

By fitting this model (Eqs. 11–15) to the experimental data, the diffusion coefficient of the carbonate ions ( $D_s$ ) and the intrinsic surface reaction rate ( $r^0$ ) under different reaction conditions can be estimated by a least square method.

$D_s$  and  $r^0$  at 873, 923, and 973 K in a gas consisting of 1800 ppmv  $\text{SO}_2$ , 3 vol %  $\text{O}_2$ , 15 vol %  $\text{CO}_2$ , and 81.8 vol %  $\text{N}_2$  are estimated first. The values of  $D_s$  and  $r^0$  at which the sum of squared deviations between the measured conversions and the model predicted conversions ( $\sum (x_{\text{Measured}} - x_{\text{Model predicted}})^2$ ) becomes least are taken as the solutions.

Figures 9 and 10 show, respectively, the plots of the obtained values of  $D_s$  and  $r^0$  (in the form of  $\ln(D_s)$  and  $\ln(r^0)$ ) against  $1/T$ . The lines in Figures 9–10 can be represented by the following expressions:

$$D_s = 4.4 \times 10^{-7} e^{\frac{-201700(\text{J/mol})}{RT}} \quad (\text{m}^2/\text{s}) \quad (16)$$

$$r^0 = 0.0045 e^{\frac{-25200(\text{J/mol})}{RT}} \quad [\text{mol}/(\text{m}^2\text{s})] \quad (17)$$

These results show that the solid-state diffusivity of carbonate ions near the calcite grain surface has an activation

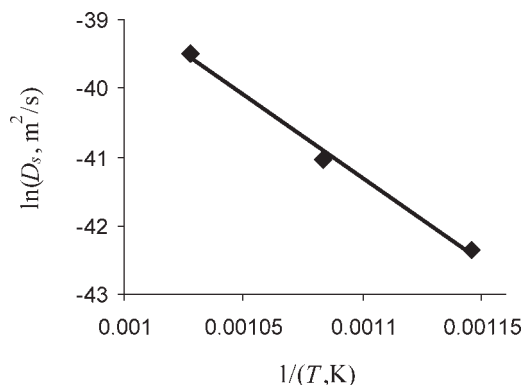


**Figure 9. Variation of solid-state diffusivity of carbonate ions in the surface layer of calcite grains with temperature in a gas consisting of 1800 ppmv  $\text{SO}_2$ , 3 vol %  $\text{O}_2$ , 15 vol %  $\text{CO}_2$ , and 81.8 vol %  $\text{N}_2$ .**

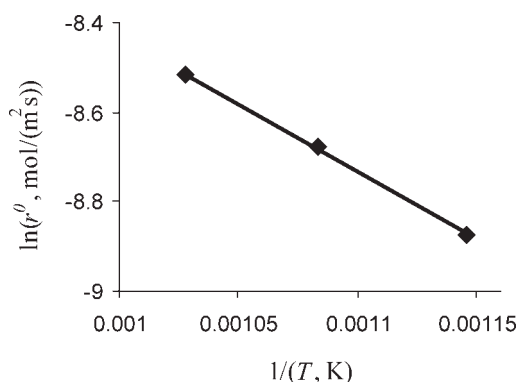


**Figure 10. Variation of intrinsic surface reaction rate with temperature in a gas consisting of 1800 ppmv SO<sub>2</sub>, 3 vol % O<sub>2</sub>, 15 vol % CO<sub>2</sub>, and 81.8 vol % N<sub>2</sub>.**

energy of about 202 kJ/mol, whereas the intrinsic surface reaction rate has an activation energy of about 25 kJ/mol.

The dependence of the intrinsic surface reaction rate on SO<sub>2</sub> and CO<sub>2</sub> concentrations is expressed by the following empirical equation:

$$r^0 = A e^{\frac{-25200(\text{J/mol})}{RT}} C_{\text{SO}_2}^n C_{\text{CO}_2}^m \quad [\text{mol}/(\text{m}^2\text{s})] \quad (18)$$

The reaction order of O<sub>2</sub> is zero in the investigated O<sub>2</sub> concentration interval. Though the insensitivity of the sulfation rate to O<sub>2</sub> in the initial period before nucleation of the solid product is well explained by the sulfation mechanism suggested by Hu et al.,<sup>16</sup> the validity of Eq. 18 at O<sub>2</sub> concentrations which are significantly lower or higher than the O<sub>2</sub> concentrations used in this study still needs to be verified by further experiments.

The reaction orders of SO<sub>2</sub> and CO<sub>2</sub> are estimated by further fitting to the conversions measured at different SO<sub>2</sub> and CO<sub>2</sub> concentrations. By assuming that the reaction orders of SO<sub>2</sub> and CO<sub>2</sub> and activation energies for both  $D_s$  and  $r^0$  do not vary with gas concentrations and the temperature, the reaction orders of SO<sub>2</sub> and CO<sub>2</sub> can also be determined by the least square method.

At fixed CO<sub>2</sub> and O<sub>2</sub> concentrations, the intrinsic surface reaction rate at a different SO<sub>2</sub> concentration can be calculated by the following equation:

$$r_2^0 = r_1^0 \left( \frac{C_{\text{SO}_2,2}}{C_{\text{SO}_2,1}} \right)^n \quad (19)$$

$r^0$  at 1800 ppmv SO<sub>2</sub> is known. By specifying  $n$ ,  $r^0$  at 900 ppmv SO<sub>2</sub> can be calculated. With known  $D_s$  and  $r^0$ , the conversion can be predicted by using the above model (Eqs 11–15). The sum of squared deviations between the model predicted conversions and the measured conversions (including data at both 873 and 973 K) is calculated. The above calculations are done at different values of  $n$ . The reaction order at which the sum of squared deviations becomes least is taken as the final solution. At fixed SO<sub>2</sub> and O<sub>2</sub> concentrations, the same procedure is used to get the reaction order of CO<sub>2</sub>.

The obtained reaction order is approximately 0.9 for SO<sub>2</sub> and approximately -0.75 for CO<sub>2</sub>. The absolute values of these two reaction orders are significantly higher than the apparent reaction orders of SO<sub>2</sub> and CO<sub>2</sub> evaluated with the measured average conversion rates.

With the obtained parameters, the expression for the intrinsic surface reaction rate can be established:

$$r^0 = 0.22 e^{\frac{-25200(\text{J/mol})}{RT}} C_{\text{SO}_2}^{0.9} C_{\text{CO}_2}^{-0.75} \quad [\text{mol}/(\text{m}^2\text{s})] \quad (20)$$

According to the expression for the intrinsic surface reaction rate in Eq. 9, the reaction orders of SO<sub>2</sub> and CO<sub>2</sub> should be dependent on their concentrations. The evaluated reaction orders are therefore a kind of averages in the used gas concentration intervals. The obtained results correspond to a relatively dominant influence of  $K_5^{-1} C_{\text{CO}_2}$  and a relatively weak influence of  $K_1 C_{\text{SO}_2}$  in the denominator of the expression for the intrinsic surface reaction rate in Eq. 9. This may partly be caused by the relatively high CO<sub>2</sub> concentrations and low SO<sub>2</sub> concentrations used in this study.

For comparison, the intrinsic surface reaction rates predicted by Eq. 20 are plotted in Figure 7 as well. The intrinsic rates predicted by Eq. 20 are generally about 2–3 times higher than the measured average rates, which is in good agreement with the conclusion of significant resistance of solid-state diffusion in the initial sulfation period.

The solid-state diffusivity of carbonate ions obtained here (for example about  $4.5 \times 10^{-19}$  m<sup>2</sup>/s at 873 K) is about three orders of magnitude higher than the self-diffusivity of carbonate ions in calcite lattice predicted by the correlation (Eq. 21) presented by Haul and Stein.<sup>37</sup>

$$D_L = 4.5 \times 10^{-8} e^{\frac{-242790(\text{J/mol})}{RT}} \quad (\text{m}^2/\text{s}) \quad (21)$$

At 873 K Eq. 21 predicts a diffusivity of about  $1.4 \times 10^{-22}$  m<sup>2</sup>/s.

The diffusion process in our case takes place only in a thin layer of about a few nm near the calcite grain surface because of the relatively low solid-state diffusivity and short reaction times. Solid-state diffusion in the grain-boundaries (the interfacial area between two crystal grains) and the surface layer of a grain was observed<sup>38–39</sup> to be up to several orders of magnitude faster than the lattice diffusion in the inner part of the grain, most likely because of the more defective nature of the surface layer of the grain than the inner part of the grain. This enhanced diffusion in grain-boundary/surface layers seems to give a good explanation of the relatively high diffusivity of the carbonate ions obtained in this study. The similar phenomenon was actually also observed by Haul and Stein.<sup>37</sup> In their experimental work to measure the lattice diffusivity of the carbonate ions in calcite, Haul and Stein<sup>37</sup> observed that the initial diffusion of carbonate ions in the surface layer of the calcite grains was significantly faster than the subsequent diffusion of the carbonate ions in the inner part of the calcite grains.

With the obtained parameters, solid-state diffusivity of carbonate ions and the intrinsic surface reaction rate can be calculated by Eqs. 16 and 20, respectively. The initial sulfation of the limestone at different conditions can thus be simulated by the model (Eqs. 11–15). As shown in Figures 3–6, the



model simulates the initial sulfation process very well, reflected by the good fit between the conversion vs. time curves calculated by the model and the measured conversions. The standard deviation between the experimentally measured conversions and the model predicted values are calculated to be about  $\pm 8.7 \times 10^{-5}$ .

For comparison, the variation of the limestone conversion with the reaction time at the three temperatures used in this study are calculated with the intrinsic rate equation presented by Hajaligol et al.,<sup>2</sup> which gives the highest rate among the literature references. Hajaligol's equation is:

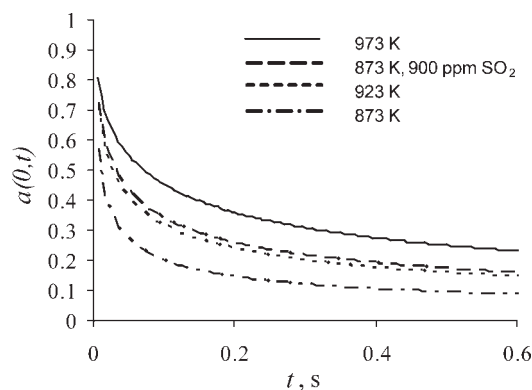
$$r^0 = 1.5e^{\frac{68650}{8.314T}}C_{\text{SO}_2} \quad (22)$$

Figure 3 shows that the conversions predicted by this equation, even without consideration of any diffusion resistance, are at least a factor 10 lower than the experimentally measured values. No fit at all to our experimental data can be claimed in any reasonable sense of the word. This demonstrates again that the intrinsic rate expressions<sup>1,2,5,13</sup> established by using the rate data at relatively higher conversions are not able to give a reasonable description of the initial sulfation kinetics of Faxé Bryozo.

As discussed earlier, the initial sulfation process most likely was significantly influenced by solid-state diffusion. With a negligible resistance of intra-particle gas phase diffusion, the sulfation process was thus under mixed control by chemical reaction and solid-state diffusion.

Fitting of the model to the experimental data resulted in activation energies of about 25 kJ/mol for the chemical reaction and about 202 kJ/mol for the solid-state diffusion of carbonate ions. The apparent activation energies calculated by using the measured average conversion rates are all significantly higher than the activation energy of 25 kJ/mol for the chemical reaction but significantly lower than the activation energy of about 202 kJ/mol for the solid-state diffusion of carbonate ions. This seems to be a good support to the conclusion of mixed control.

The mixed control mechanism seems also to give a satisfactory explanation of the significantly lower apparent reaction orders of SO<sub>2</sub> and CO<sub>2</sub> than their intrinsic reaction orders. Figure 11 shows the variation of  $a(0,t)$  with reaction time at different temperatures and SO<sub>2</sub> concentrations calculated by the model. This figure demonstrates that the carbonate ion concentration at the calcite grain surface decreases exponentially with time. The decrease is significantly slower at higher temperatures, caused by a decrease in the relative control by solid-state diffusion because of the significantly higher activation energy of solid-state diffusion than that of the chemical reaction. As it is seen in this figure, a decrease in SO<sub>2</sub> concentration creates a similar effect as an increase in the temperature. The slower decrease in the carbonate ion concentration at the calcite grain surface at a lower SO<sub>2</sub> concentration is caused by an increase in the relative control by chemical reaction because of a decreased chemical reaction rate. This slower decrease in the carbonate ion concentration at the calcite grain surface at a lower SO<sub>2</sub> concentration compensates partly the effect of the lowered SO<sub>2</sub> concentration on the rate of the chemical reaction, which is thus most likely the reason for the low apparent reaction orders.



**Figure 11. Model calculated variation of the dimensionless carbonate ion concentration at the calcite grain surface with reaction time at different temperatures and SO<sub>2</sub> concentrations (standard conditions if not specified:  $P$ : 0.1 MPa; inlet SO<sub>2</sub>: 1800 ppmv; O<sub>2</sub>: 3 vol %; CO<sub>2</sub>: 30 vol %; N<sub>2</sub>: balance).**

## Conclusion

The initial kinetics of the direct sulfation of Faxé Bryozo, a porous bryozoan limestone has been studied in a pilot entrained flow reactor at temperatures around 873–973 K and a reaction time less than 0.6 s. The initial sulfation process is shown to be promoted by higher SO<sub>2</sub> concentrations, lower CO<sub>2</sub> concentrations, and higher temperatures. O<sub>2</sub> has little influence on the initial sulfation process. The initial sulfation process is also shown to be significantly (more than a couple of orders of magnitude) faster than the further sulfation after the initiation of nucleation and crystal growth of anhydrite, the solid product.

The initial sulfation of the limestone is most likely controlled by both the chemical reaction at the calcite grain surface and solid-state diffusion in the grain. A theoretical reaction-diffusion model based on the balance between the sulfation reaction at the calcite grain surface and the solid-state diffusion of carbonate ions in the grain gives a satisfactory description of the kinetics of the initial sulfation process. The intrinsic kinetics of the direct sulfation of the limestone, assessed by model simulation, has an activation energy of about 25 kJ/mol and the reaction orders of 0.9,  $-0.75$ , and zero for SO<sub>2</sub>, CO<sub>2</sub>, and O<sub>2</sub>, respectively.

The solid-state diffusivity of the carbonate ions in the thin layer near the calcite grain surface, estimated by the model simulation at temperatures around 873–973 K, has an activation energy of about 202 kJ/mol and is about three orders of magnitude higher than the diffusivity of carbonate ions in the inner lattice of the calcite grains. This enhanced diffusion at the calcite grain surface is most likely related to the more defective nature of the surface layer than the inner part of the calcite grain.

The experimental results obtained in this study indicate also that the kinetic behaviors of the direct sulfation of limestone in the initial period and the subsequent period with crystal growth of the solid product are very different. It may be not appropriate to assess the intrinsic kinetics of the direct sulfation of limestone by direct use or extrapolation of the

rate data measured in the period with crystal growth of the solid product. However, assessing the intrinsic kinetics by model simulation has its limitations as well because of its dependency on the theory. Even though the experimental observations are explained well by the theories proposed in this study and in Hu et al.,<sup>16</sup> and even though the experimental results are described very well by the model which is established according to the proposed theory, the correctness of the declaration of our fitted kinetic parameters as the intrinsic still needs to be further verified by experimental results in the future.

## Acknowledgments

This work is carried out in CHEC (Combustion and Harmful Emission Control) Research Center funded a.o. by the Technical University of Denmark, the Danish Technical Research Council, the European Union, the Nordic Energy Research, Dong Energy A/S, Vattenfall A.B., F L Smidth A/S, and Public Service Obligation funds from Energinet.dk and the Danish Energy Research program. The work is financially supported by FLSmidth A/S and the Technical University of Denmark.

## Notation

$A$  = constant,  $\text{mol}^{(1-n-m)}/(\text{m}^{(2-3(n+m))}\text{s})$   
 $a$  = dimensionless concentration of carbonate ions (ratio between actual carbonate ion concentration and carbonate ion concentration in pure calcite crystal)  
 $C$  = concentration,  $\text{mol}/\text{m}^3$   
 $D$  = diffusion coefficient,  $\text{m}^2/\text{s}$   
 $E_a$  = activation energy,  $\text{kJ}/\text{mol}$   
 $K_1$  = equilibrium constant for  $\text{SO}_2$  adsorption,  $\text{m}^3/\text{mol}$   
 $K_5$  = equilibrium constant for  $\text{CO}_2$  desorption,  $\text{mol}/\text{m}^3$   
 $k$  = reaction rate constant (unit depending on rate expressions)  
 $l$  = diffusion distance,  $\text{m}$   
 $M$  = molar weight,  $\text{g}/\text{mol}$   
 $Nm^3$  = cubic meter at standard conditions (273.15 K, 101325 Pa)  
 $P$  = total pressure,  $\text{Pa}$   
 $\text{ppmv}$  = ppm on volume basis  
 $R$  = gas constant,  $\text{J}/(\text{mol K})$   
 $r$  = surface reaction rate,  $\text{mol}/(\text{m}^2\text{s})$   
 $S_t$  = total surface area,  $\text{m}^2/\text{g}$   
 $t$  = reaction time,  $\text{s}$   
 $T$  = temperature,  $\text{K}$   
 $V$  = gas flow,  $\text{m}^3/\text{s}$   
 $w$  = solid feeding rate,  $\text{g}/\text{s}$   
 $x$  = conversion of solid reactant (limestone), dimensionless  
 $y$  = molar fraction, dimensionless  
 $\eta$  = fraction of  $\text{CaCO}_3$  in limestone  
 $[ ]_v$  = vacant active sites  
 $[\text{SO}_2]_v$  = active sites occupied by  $\text{SO}_2$   
 $[\text{CO}_2]_v$  = active sites occupied by  $\text{CO}_2$   
 $[\text{SO}_3^{2-}]$  = carbonate sites in calcite lattice occupied by sulfite ions  
 $[\text{SO}_4^{2-}]$  = carbonate sites in calcite lattice occupied by sulfate ions

## Superscript

0 = intrinsic, pure  
 $n, m$  = reaction order  
 $s$  = surface

## Subscript

$s$  = solid state

## Literature Cited

- Snow MJH, Longwell JP, Sarofim AF. Direct sulfation of calcium carbonate. *Ind Eng Chem Res.* 1988;27:268–273.
- Hajaligol MR, Longwell JP, Sarofim AF. Analysis and modeling of the direct sulfation of  $\text{CaCO}_3$ . *Ind Eng Chem Res.* 1988;27:2203–2210.
- Iisa K, Hupa M, Yrjas P. Product Layer Diffusion in the Sulfation of Calcium Carbonate. In: *Twenty-Fourth Symposium (International) on Combustion/The Combustion Institute*, Philadelphia, PA: The Combustion Institute, 1992: 1349–1356.
- Iisa K, Hupa M. Rate-limiting processes for the desulfurization reaction at elevated pressures. *J Inst Energ.* 1992;65:201–205.
- Fuertes AB, Velasco G, Fuente E, Parra JB, Alvarez T. Sulfur retention by limestone particles under PFBC conditions. *Fuel Process Technol.* 1993;36:65–71.
- Fuertes AB, Velasco G, Fuente E, Alvarez T. Study of the sulfation of limestone particles at high  $\text{CO}_2$  partial pressure. *Fuel Process Technol.* 1994;38:181–192.
- Illerup JB, Dam-Johansen K, Lunden K. High-temperature reaction between sulfur dioxide and limestone-VI. The influence of high pressure. *Chem Eng Sci.* 1993;48:2151–2157.
- Krishnan SV, Sotirchos SV. Sulfation of high purity limestones under simulated PFBC conditions. The can. *J Chem Eng.* 1993;71: 244–255.
- Tullin C, Nyman G, Ghardashkhani S. Direct sulfation of  $\text{CaCO}_3$ : the influence of  $\text{CO}_2$  partial pressure. *Energy Fuels.* 1993;7:512–519.
- Zhong Q. Direct sulfation reaction of  $\text{SO}_2$  with calcium carbonate. *Thermochim Acta.* 1995;260:125–136.
- Zevenhoven R, Yrjas P, Hupa M. Sulfur dioxide capture under PFBC conditions: the influence of sorbent particle structure. *Fuel* 1998;77:285–292.
- Alvarez E, Gonzalez JF. High pressure thermogravimetric analysis of the direct sulfation of Spanish calcium-based sorbents. *Fuel* 1999; 78:341–348.
- Liu H, Katagiri S, Kaneko U, Okazaki K. Sulfation behaviour of limestone under high  $\text{CO}_2$  concentration in  $\text{O}_2/\text{CO}_2$  coal combustion. *Fuel* 2000;79:945–953.
- Qiu K, Lindqvist O. Direct sulfation of limestone at elevated pressures. *Chem Eng Sci.* 2000;55:3091–3100.
- Hu G, Dam-Johansen K, Wedel S, Hansen JP. Review of the direct sulfation reaction of limestone. *Prog Energy Combust Sci.* 2006; 32:386–407.
- Hu G, Dam-Johansen K, Wedel S, Hansen JP. Direct sulfation of limestone. *AIChE J.* 2007;53:958–960.
- West AR. *Basic Solid State Chemistry*. Chichester: Wiley, 1999.
- Dam-Johansen K. *Absorption of  $\text{SO}_2$  on Dry Limestones*. Ph.D. Thesis (in Danish), Department of Chemical and Biochemical Engineering, Technical University of Denmark, 1987.
- Dam-Johansen K, Østergaard K. High-temperature reaction between sulfur dioxide and limestone-I. Comparison of limestone in two laboratory reactors and a pilot plant. *Chem Eng Sci.* 1991;46:827–837.
- Dam-Johansen K, Østergaard K. High-temperature reaction between sulfur dioxide and limestone-II. An improved experimental basis for a mathematical model. *Chem Eng Sci.* 1991;46:839–845.
- Dam-Johansen K, Hansen PFB, Østergaard K. High-temperature reaction between sulfur dioxide and limestone-III. A grain-micro-grain model and its verification. *Chem Eng Sci.* 1991;46:847–853.
- Dam-Johansen K, Østergaard K. High-temperature reaction between sulfur dioxide and limestone-IV. *Chem Eng Sci.* 1991;46:855–859.
- Froment GF, Bischoff KB. *Chemical Reactor Analysis and Design*. New York: Wiley, 1990.
- Fuller EN, Giddings JC. A comparison of methods for predicting gaseous diffusion coefficients. *J Gas Chromatogr.* 1965;3:322.
- Fuller EN, Schettler PD, Giddings JC. A new method for the prediction of binary gas-phase diffusion coefficients. *Ind Eng Chem.* 1966; 58(5):18–27.
- Perry RH, Green DW, Maloney JO. *Perry's Chemical Engineers' Handbook, 6th ed.* New York: McGraw-Hill Book Company, 1984.
- Beruto D, Giordani M, Botter R. Microstructure development of  $\text{Li}_2\text{CO}_3$ - $\text{CaCO}_3$  eutectic mixture in  $\text{CO}_2$  (g) and  $\text{N}_2$  (g) environment. *J. Physique, Colloque C1*, 1986;47(Suppl 2):527–531.
- Tetard F, Bernache-Assollant D, Champion E. Pre-eutectic densification of calcium carbonate doped with lithium carbonate. *J Therm Anal Calorimetry.* 1999;56:1461–1473.
- Labotka TC, Cole DR, Riciputi LR, Fayek M. Diffusion of C and O in calcite from 0.1 to 200 MPa. *Am Mineral.* 2004;89:799–806.
- Frenkel Y. Thermal agitation in solids and liquids. *Z Phys.* 1926; 35:652–669.
- Wagner C, Schottky W. Theorie der geordneten Mischphasen. *Z Phys Chem B.* 1930;11:163–210.

32. Manning JR. *Diffusion Kinetics for Atoms in Crystals*. Princeton: D. Van Nostrand Company, Inc., 1968.
33. Hayes W, Stoneham AM. *Defects and Defect Processes in Nonmetallic Solids*. New York: Wiley, 1985.
34. Kirkaldy JS, Young DJ. *Diffusion in the Condensed State*. London: The Institute of Metals, 1987.
35. Tilley RJD. *Defect Crystal Chemistry and Its Application*. Glasgow: Blackie & Son Limited, 1987.
36. Glicksman ME. *Diffusion in Solids: Field Theory, Solid-State Principle, and Applications*. New York: Wiley, 2000.
37. Haul RAW, Stein LH. Diffusion in calcite crystals on the basis of isotopic exchange with carbon dioxide. *Trans Faraday Soc.* 1955;51: 1280–1290.
38. Barnes RS. Diffusion of copper along the grain boundaries of nickel. *Nature*. 1950;166:1032–1033.
39. Hoffman RE, Turnbull D. Lattice and grain boundary self-diffusion in silver. *J Appl Phys*. 1951;22:634–639.

*Manuscript received Aug. 28, 2007, and revision received Apr. 27, 2008.*